SOLID STATE PHOTOELECTROCHEMICAL SOLAR ENERGY CONVERSION BASED ON A MIXTURE OF *MEH-PPV* AND *MDMO-PPV*

BY: **ANTENEH WODAJE BAYEH**

A thesis submitted in partial fulfillment of the requirement for the degree of Master of Science in Materials Science at Addis Ababa University School of Graduate Studies

Addis Ababa, Ethiopia

June 2010

ADDIS ABABA UNIVERSITY

GRADUATE STUDIES

SOLID STATE PHOTOELECTROCHEMICAL SOLAR ENERGY CONVERSION BASED ON MIXTURE OF MDMO-PPV and MEH-PPV

By: **ANTENEH WODAJE BAYEH**

Materials Science Program

Faculty of Science

Approved by the Examining Board

Prof. Teketel Yohannes _____

(Advisor)

D.r S.K Ghoshal _____

(Examiner)

D.r Mesfin Redi _____

(Examiner, Chairperson)

Acknowledgement

I offer my deepest gratitude and special affection to my advisor Prof. Teketel Yohannes for his generous advise, devoted assistance, encouragement in all stages of the work, constant guidance and constructive criticism which were necessary for the progress of the research.

I would like to express my thanks to my wife Tsigereda Kassa for her encouragement. I would like to express my thank Ato Sisay Tadesse, Ato Getachew Adam and Ato Siraye Esubalew for the concern they shown, and the suggestions and encouragement, which I have got in the work.

Table of Contents

List of tables

List of figures

Abstract

Solid state photoelectrochemical solar energy conversion based on a mixture of MEH-PPV and MDMO-PPV, coated on ITO glass as light harvesting unit, a solid polymer electrolyte, POMOE complexed with I_3^- /I^- redox couple and oxidized PEDOT as counter electrode have been fabricated and studied for its photoresponse behavior. The short circuit current (I_{sc}), open circuit voltage (V_{oc}), and fill factor (FF) of this mixed polymer based PEC is higher than that of MEH-PPV based device. A PEC with a structure ITO │ (MEH-PPV:MDMO-PPV) │ POMOE │: I_3^- /I^- │ PEDOT │ ITO produce V_{oc} of 289.7 mV, I_{sc} of 0.21 μA/cm^2 and FF of 0.32. The device showed an incident monochromatic photon to current conversion efficiency (IPCE) of 0.0034% illuminated from front side and 0.00013% illuminated from back side. The dependence of I_{sc} and V_{oc} on incident light intensity showed both I_{sc} and V_{oc} increases with increasing light intensity. The plot of $\log I_{sc}$ versus $\log P_i$ yielded straight line with the power factor α is equal to 0.793. Our results show that mixing of two donor type polymer, PEC show relatively improved performance when compared with individual MEH-PPV based device.

Declaration

This thesis is my original work and has not been presented for a degree in any University.

Name: _____

Signature: _____

This thesis has been submitted for examination with my approval as a university advisor.

_____

Prof. Teketel Yohannes

_____

Date

1. INTRODUCTION

Mankind is still searching for reliable, cheap and environmentally friendly energy sources. The classical energy sources cannot provide these requirements for the future any more. The fossil energy sources coal, oil and gas cause air pollution and climate problems. Carbon dioxide, the final product of the combustion of all organic materials, is known to influence earth climate significantly. Also, the stock of these carbon-based fuels is limited and thought to run out in roughly 50 years [1].

The use of nuclear power as energy source is not accepted by wide section of the population anymore because of security and health risk. Further, the disposal of nuclear waste is still an unsolved problem, worldwide. Over the last decades, there have been big efforts for developing new, alternative energy sources. The sun, on the other hand, matches all requirements of an ideal energy source. It is reliable, ubiquitous and is free. The nature uses the sun as its only energy source in photosynthesis since millions of years.

The direct conversion of sunlight into electricity by photovoltaic cells is known for many years. Monocrystalline silicon and gallium arsenide devices exceed efficiencies of 24% energy conversion [1] of the terrestrial sunlight, but the production costs are too high for economic use in widespread energy production. Thin film technique should reduce material consumption and production costs. Typical materials, which are used in thin film photovoltaic devices, are inorganic semiconductors like amorphous and polycrystalline silicon, cadmium telluride and copper indium diselenide. Generally, all these inorganic semiconductors need high temperature operations in their production, which causes high cost, and are difficult to handle.

Conjugated polymers have been extensively studied in the last two decades because their properties suggest their use in several potential applications [2]. The reversible change from a metallic conductor to a semiconductor material by electrochemical doping/undoping makes possible the application of these materials in different electronic devices, including photovoltaic and photoelectrochemical cells [3].

Several works have demonstrated the photoeffects produced by illuminating the heterojunction formed at the interface between an electrolyte and conducting polymers, such as polyaniline [4], polypyrrole [5] and polythiophene [6]. The quantum yield of solar cells based on these materials is lower than that obtained with conventional inorganic semiconductor solar cells [7]; however, efforts have been done to improve the photoeffects in organic materials due to the possibility of achieving inexpensive and flexible devices with different shapes and sizes [7].

One variety of polymer solar cells that has recently been studied extensively consists of donor–acceptor heterojunctions between conjugated polymers and fullerenes or its derivatives [6]. Device efficiency was further improved by using an interpenetrating, rather than a planar, donor/acceptor network throughout the device, thereby substantially increasing the interface area and therefore exciton breakdown.

The regenerative photoelectrochemical solar cells based on conducting polymers are regarded as a potentially low-cost alternative to conventional solid-state devices since 1991[3]. Commonly the use of liquid electrolyte limits the application of this system. The PEC solar cells using liquid electrolyte show excellent power conversion performance, however, their commercial application is still limited due to stability problems as well as technological aspects of the large module production. Therefore, replacing the liquid electrolyte with solid-state analog allows the assembly of all-solid-state PEC devices to eliminate practical problems with sealing and degradation. Solid-state PEC solar energy conversion using conjugated polymers as photoactive electrodes and a solid polymer electrolyte mixed with a redox couple has been investigated [3].

In this thesis, the photoelectrochemical and optical properties of solid-state PEC were studied. The PEC contained a film of mixture of poly[2-methoxy-5-(3,7-dimethyloctyloxy)]-1,4-phenylenevinylene, (MDMO-PPV) and poly[2-methoxy-5-(2'-ethylhexyloxy)-1,4 phenylenevinylene, (MEH-PPV) coated on indium doped tin oxide (ITO) coated glass light harvesting unit (photoactive electrode); a solid polymer electrolyte poly[oxymethylene-oligo(oxyethylene)], POMOE, complexed with an I_3^-/I^- redox couple; and oxidized poly(3,4-ethylene dioxythiophene), PEDOT, coated electrochemically on ITO-coated glass counter electrode.

2. Literature Review

2.1 Electronically Conducting Polymers

One class of the organic compounds, which effectively transport charges, is electronically conducting polymers [8]. Electronically conducting polymers contain π-electron backbone, which is responsible for their unusual electrochemical properties (high electrical conductivities, low ionization potentials and high electron affinities) and optical properties (low energy optical transitions), previously observed in inorganic materials [9]. In the neutral (undoped) state these materials are insulators or semiconductors. The electronic conductivity of the material is enhanced when it is doped [10, 11]. Thus, it is possible to control the electrical conductivity of the polymer from insulating to high conducting (metallic) state.

A key discovery in the development of electronically conducting polymers was the finding in 1973 that the inorganic polymer poly-sulfur nitride, $(SN)_x$, is a metal [12]. The metallic property of $(SN)_x$ is an intrinsic property of the material related with the presence of one unpaired electron per unit. In 1976, it was found that the room temperature conductivity of $(SN)_x$ can be enhanced by an order of magnitude following exposure to bromine and similar oxidizing agents [13].

The major breakthrough in the area of electronically conducting polymers occurred later in 1977 when Shirakawa, together with MacDiarmid and Heeger [14], discovered that the conductivity of that insulating polyacetylene, which had conductivity lower than 10^{-5} S/ cm, could be increased up to 10^3 S/cm at room temperature by chemical oxidation with iodine or AsF_5. Further improvements in polymerization methods produced polymers containing fewer defects in their structure and having conductivity as high as 1.5×10^5 S/cm [15].

2.1.1 The Concept of Doping As Applied To Conjugated Polymers

Chemically produced conjugated polymers are semiconductors/insulators after the cleaning steps. Their metal like properties, i.e. their high conductivity, arises only after ´doping´, concomitant with a change of the redox state of the polymer.

The term ´doping´ is generally correct, as a small quantity of a dopant gives rise to disproportionally large changes of the properties of the material.

In silicon, as an example for an inorganic semiconductor, the dopant occupies positions within the lattice of the host material. This results in an either electron-rich (i.e. phosphorus as dopant) or electron-deficient (i.e. boron as dopant) site, with no charge transfer taking place between the two species. The effect of doping is due to the amount of the valence electrons of the dopant and the host material. As silicon has four valence electrons, replacement with boron with only three valence electrons results in electron-deficiency, whereas doping with phosphorus with five valence electrons gives electron-rich sites as shown below.

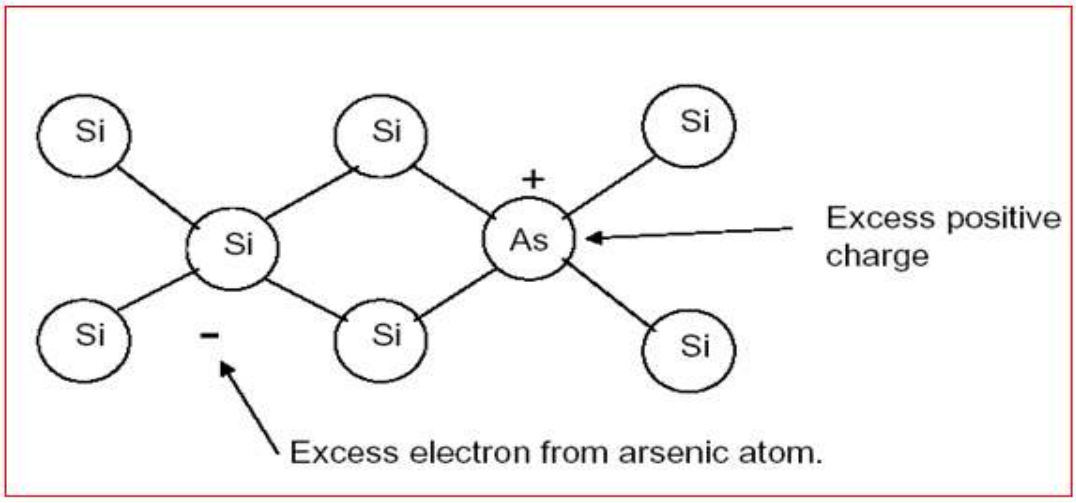

Figure 2.1. Substitutional doping in silicon. In this example, arsenic (As) is an n-type dopant.

In contrast to this, the doping of conjugated polymers [16, 17] is essentially a charge transfer reaction that results in a partially oxidized or reduced polymer rather than the creation of holes or electrons.

It can be done chemically with reducing (Donor, D, n-doping) or oxidizing (Acceptor, A, p-doping) agents or electrochemically by applying a certain voltage. Oxidation in this context is referred to as p-doping. The basic processes are shown in reactions (1).

P-doping:

$$(\pi\text{-polymer}) + [Li^{+}(BF_4^{-})] \quad \Longrightarrow \quad [(\pi\text{-polymer})^{x+}(BF_4^{-})_x] + xLi^{+} + xe^{-} \qquad (1)$$

Similarly n-doping results in partial reduction of the polymer chain, as shown in reactions (2).

n-doping:

$$(\pi\text{-polymer}) + x e^{-} + [Li^{+}(BF_4)^{-}] \Longrightarrow [(\pi\text{-polymer})^{x-}(Li^{+})_x] + x(BF_4)^{-} \quad (2)$$

Chemical and electrochemical doping generally gives similar results on the properties of the induced charges. The main advantage of electrochemical doping over the chemical way lies in the control of the doping level [18]. This can easily be done electrochemically via the applied voltage giving highly reproducible results, whereas with chemical doping attempts to reach intermediate doping levels often result in inhomogeneous doping.

2.1.2 Charge Carriers

General introduction

In conjugated polymers with only carbon atoms two of the three p-orbitals of carbon are in the three-sp^2 hybrid orbitals [19]. Of these, two are used for the σ bonds of the polymer backbone, while the third forms a bond to hydrogen or any other substituent.

The so far unused third p-orbital, the p_z-orbital, gives rise to an extended π-system along the chain, which gives conjugated polymers their unique properties [20]. The bond formation is depicted in Figure 2.2 for the example of trans-polyacetylene.

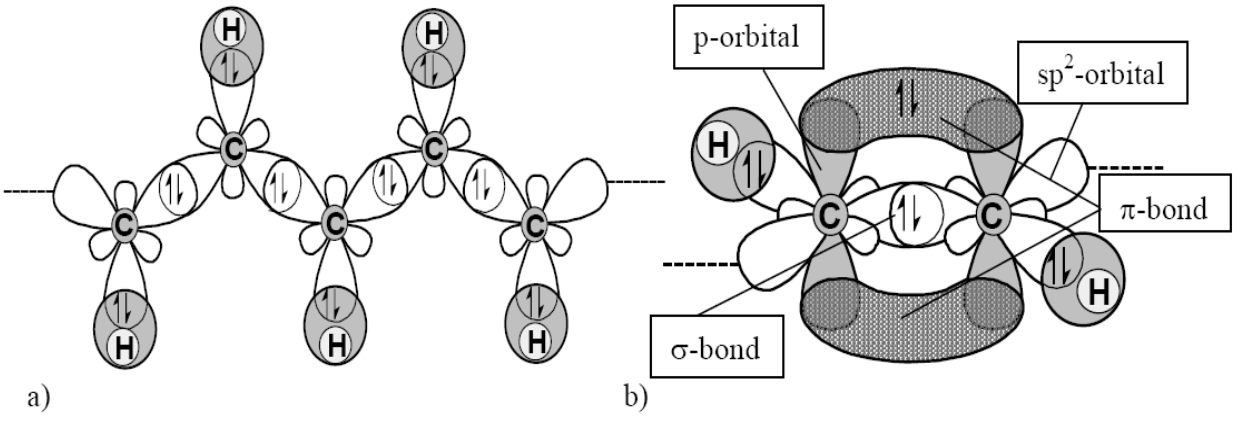

Figure 2.2. a) Formation of σ-bonds in polyacetylene by overlapping of sp^2- (carbon) and 1s- (hydrogen) orbitals; b) Formation of π-bonds through overlap from the side of the p_z-orbitals [15].

Principally, this should give a metallic material with a half-filled conduction band if all bonds were of equal length. But due to the Peierls distortion [21] dimerization occurs that breaks the symmetry of the polymer chain. In this dimerized form the π-electrons are concentrated between alternate pairs of carbon atoms, which is consistent with the observation of alternation of double and single or shorter and longer bonds along the chain. The lowering of the symmetry takes place to minimize the ground state energy.

Due to this lowering of the ground state the π-orbital is split into a filled π-orbital (HOMO, valence band, bonding orbital) and an empty π^*- orbital (LUMO, conduction band, antibonding orbital) with a certain energy gap between, the so called π-π^* band gap, which is characteristic for semiconducting materials and lies in the range of 1 to 4 eV for conjugated polymers and is an essential point for device applications. This value of the band gap varies depending on several parameters and can be controlled to a certain extent chemically [22].

Equation (3) describes the band gap in the bulk as the sum of five contributions. Figure 2.3 shows the structural meanings on the example of poly(p-phenylene).

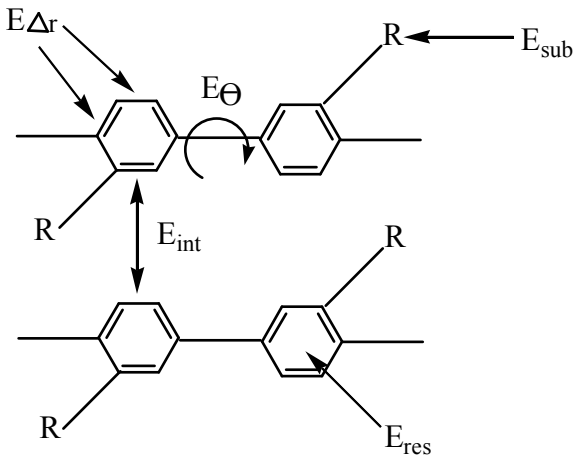

Figure 2.3. The different parameters determining the band gap of conjugated polymers in the solid state shown on the example of poly(p-phenylene): bond length alternation, $E_{\Delta r}$, resonance energy, E_{Res}, inter ring torsion angle, E_{θ}, substituent effects, E_{Sub}, and inter chain coupling ,E_{int}.

$$E_g = E_{\Delta r} + E_{res} + E_{\theta} + E_{sub} + E_{int} \quad (3)$$

Where: $E_{\Delta r}$ is the energy contribution of the bond length alternation, E_{res} is the resonance stabilization energy, E_{θ} the energy contribution caused by the inter ring torsion angle, E_{sub} the influence of substituents and E_{int} the intermolecular or inter chain coupling in the solid state.

Solitons:

Trans-polyacetylene is a polymer with a degenerate ground state since the double and single bonds can be interchanged without changing the ground state energy. Therefore the ground state has two configurations with the same energy as shown in Figure 2.4.

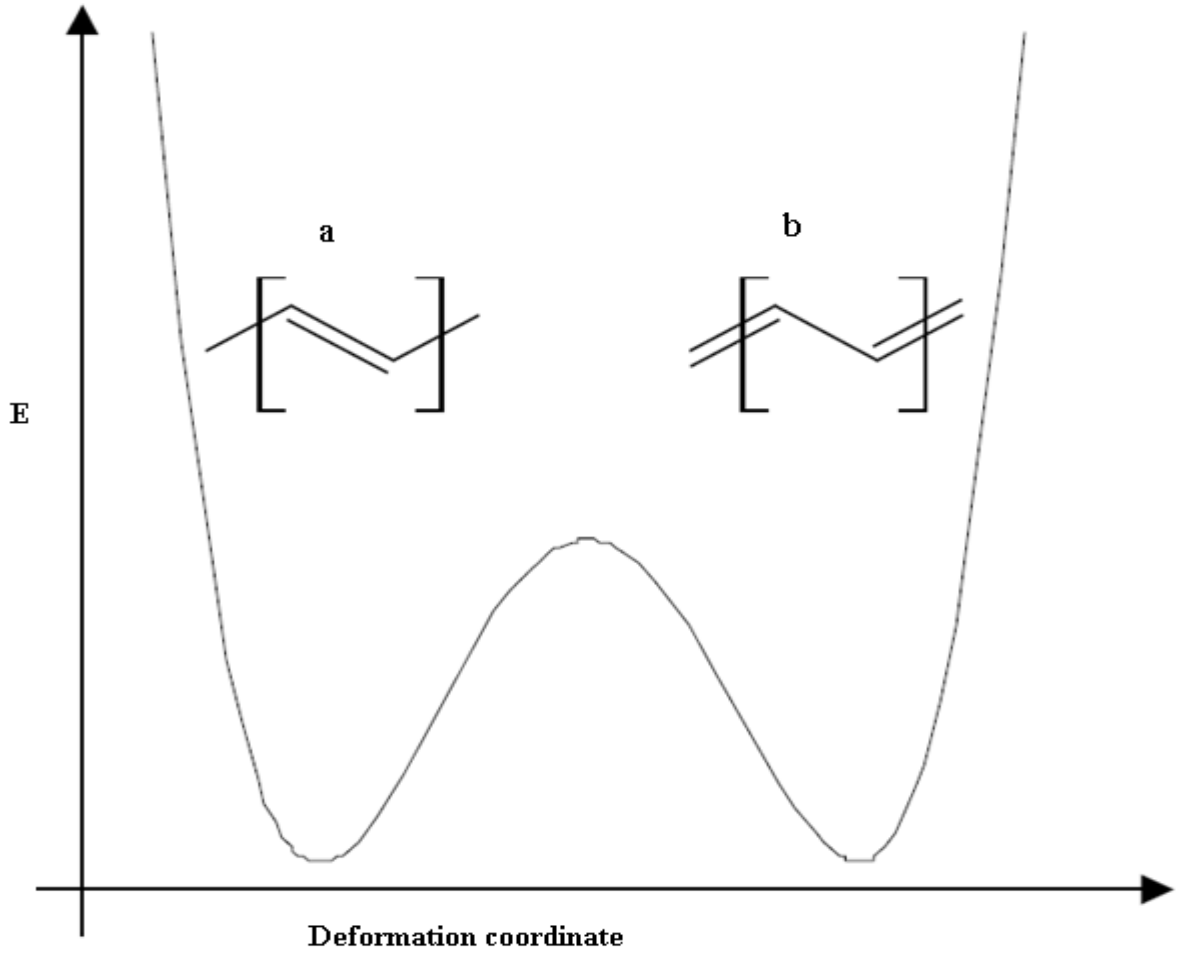

Figure 2.4. Potential energy curve for trans-polyacetylene showing the two equivalent structures a and b [23].

If both of the energetically equivalent configurations coexist on the same chain a structural defect will occur at their interface. This defect is called a (neutral) soliton; it consists of a single unpaired electron that can extend over approximately ten carbon atoms [23]. One new localised electronic state is formed in the middle of the π-π^* band gap, which can accommodate up to two electrons.

Doping adds or removes an electron to or from this state during n- or p-doping leading to a negatively or positively charged soliton, which can also be called spinless anion or cation. A band diagram for neutral, positive and negative soliton is shown in Figure 2.5.

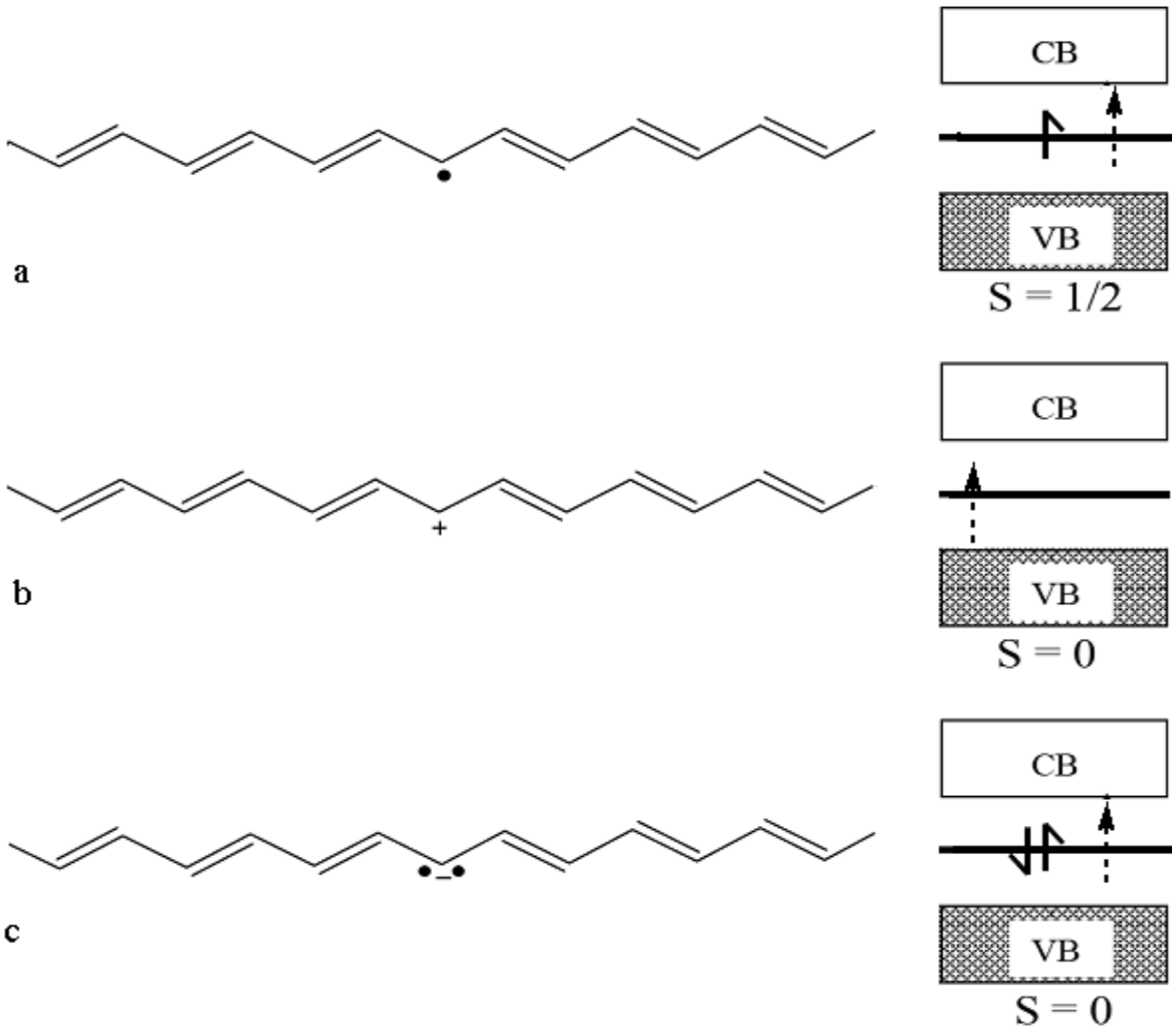

Figure 2.5. Soliton structures in polyacetylene and corresponding electronic states in the band gap, a) neutral soliton, b) positive soliton, c) negative soliton; only the neutral soliton carries a spin (S), dotted arrows indicate optical transitions to and from the mid-gap state [23].

Associated with these three types of solitons new optical transitions depending on their symmetry allowance can be observed in optical absorption spectra, which are indicated with dotted arrows.

Polarons and bipolarons:

Most other conjugated polymers have two energetically inequivalent bond alternation structures, which mean they have a non-degenerate ground state [24].

For example in poly(p-phenylenevinylene), the quinoid structure (b) is less stabilized and therefore higher in energy than the benzenoid form (a) Figure 2.6 shows the energy diagram for these two structures.

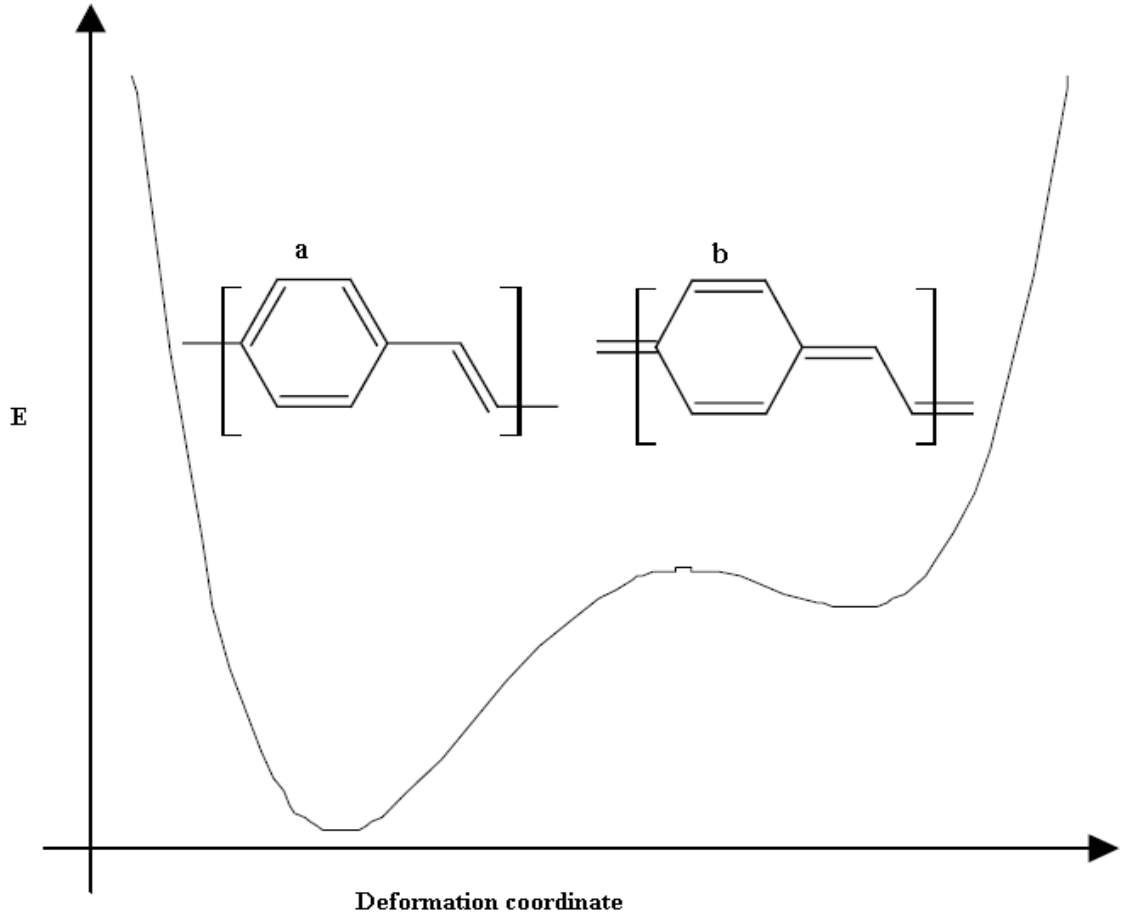

Figure 2.6. Potential energy curve for poly(p-phenylenevinylene) with its energetically inequivalent structures, (a) benzenoid and (b) quinoid [23]

A defect region will be created in the presence of charge carriers between uncharged benzenoid parts on the conjugated polymer.

Upon p- or n-doping charge carriers called polarons (radical cation or anion) and bipolarons (spinless dication or dianion) are formed and two new electronic states are created in the π-π^* band gap. A band scheme of the above described is given in Figure 2.7. The dotted arrows indicate new possible optical transitions, depending whether they are allowed by symmetry or not.

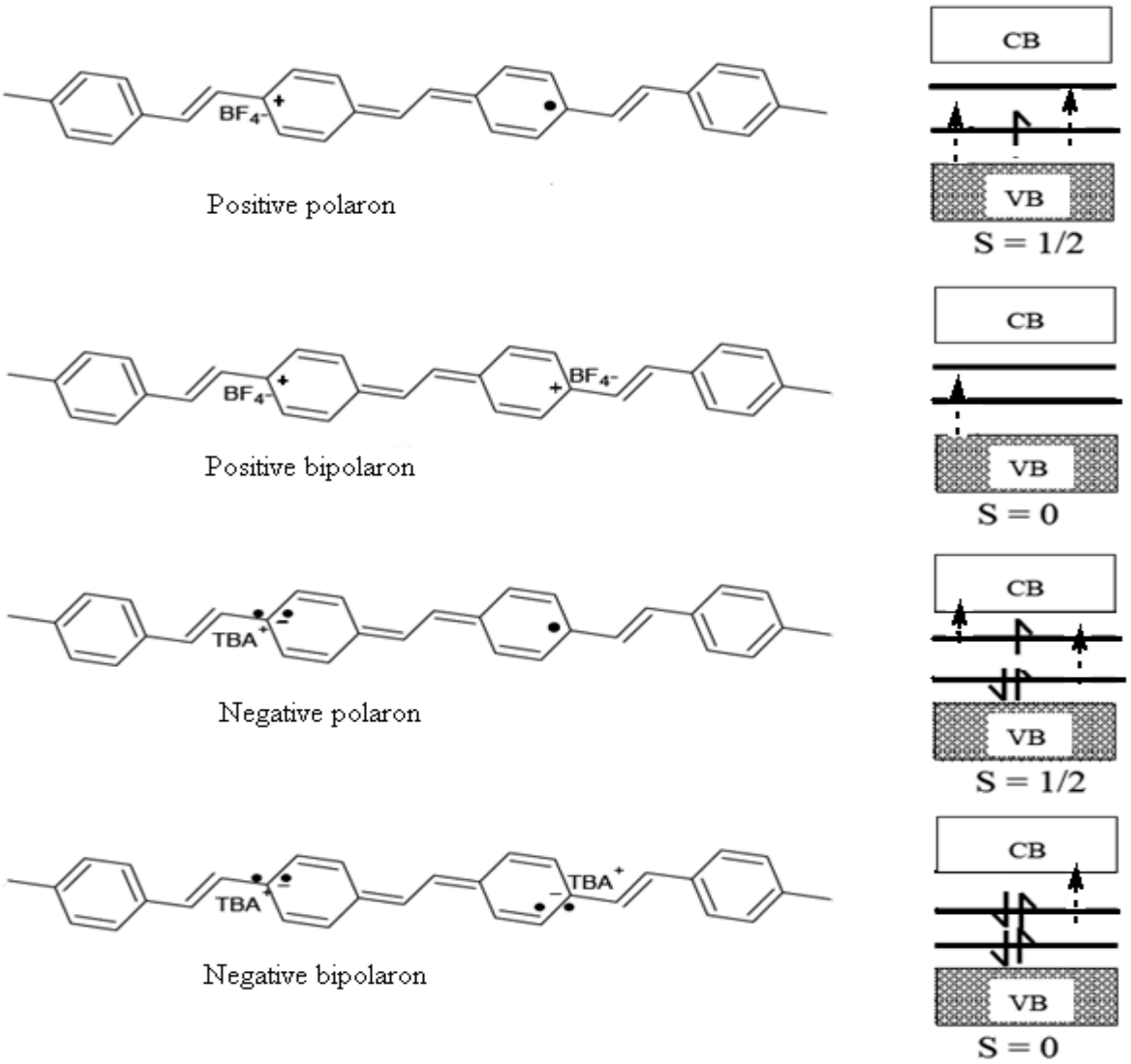

Figure 2.7. Polaron and bipolaron structures in poly(p-phenylenevinylene) with their corresponding electronic states in the band gap; only positive and negative polaron carry a spin (S). Dotted arrows indicate possible optical transitions to and from the mid-gap states [24].

Calculations show that the removal of an electron (p-doping) leads to the formation of a positive polaron (radical cation) whose associated quinoid geometry relaxation extends over three phenyl rings [25].

For removing a second electron from the polymer chain when doping proceeds two possibilities are given. The first possibility is that a second polaron will be created anywhere along the chain leading to two polarons. The second possibility is that the second electron is removed from the already existing polaron giving rise to a bipolaron.

For both processes the formation energies are predicted to be roughly the same, but the ionisation energy for bipolaron formation should be substantially lower. Therefore one bipolaron is thought to be thermodynamically more stable than two coexisting polarons [24], despite the coulombic repulsion, which is screened to a large extent by the counterions near the charge carrier introduced upon chemical or electrochemical doping.

2.1.3 Charge Transport Mechanism

The prerequisite for charge transport is the presence of mobile charge carriers. In conducting polymers the conductivity is the presence of solitons, polarons and bipolarons, which are formed by self-localization of the carriers, induced into the π-electronic systems through doping and in some cases during synthesis [26]. Conductivity of materials depends on temperature. The temperature dependence of polymer conductivity is manifested opposite to that of metals as shown below.

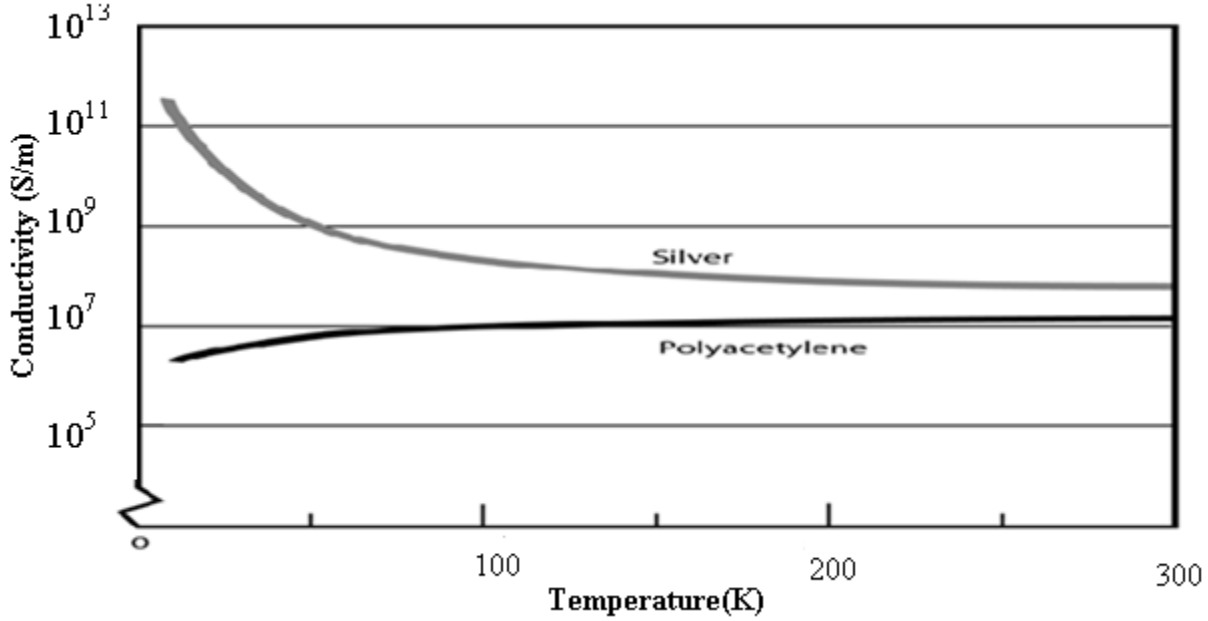

Figure 2. 8. The temperature dependence of polyacetylene and silver conductivity [14].

In case of conjugated polymers conductivity depends on doping level. Scientists noted that upon increasing the doping level, the conductivity rises by many orders of magnitude, but, there is no sharp transition from an insulating to a metallic state [27]. Besides doping, conductivity highly depends on the temperature. For metals conductivity increases with decreasing temperature. This is because of the fact that lattice vibrations freeze out as the temperature decreases to absolute zero. While in inorganic semiconductors, conductivity decreases drastically with decreasing temperature. It plays a major role in exciting the electrons from the valence band to the conduction band and hence the conductivity of inorganic semiconductors is greatly affected by temperature. But, the conductivity of doped conjugated polymers decreases if the temperature decreases, but slower than exponentially.

The effect of temperature on the conductivity is analyzed based on the doping level. For highly doped samples, the conductivity varies only slightly with the temperature, where as for low doping levels the temperature dependence is very drastic.

There is no definite mechanism of charge transport and hence different models are suggested over the whole conductivity range. In the undoped form of conjugated polymers, the charge transport is similar to that of amorphous semiconductors. It is explained by hopping between localized states. At very low doping levels, the conductivity is mainly due to hopping (phonon assisted quantum mechanical tunneling). Its concept is generally deduced from ionic conduction to electronic conduction in amorphous and disordered non-metallic solids and polymers. In such materials we do not have free charge carriers, rather than localized electrons and so they can move between these localized states which are distributed randomly.

For polyacetylene, where solitons are dominant charge carriers, intersoliton hopping is the dominant conductivity mechanism. The solitons may be either neutral or charged, see Figure 2.9.

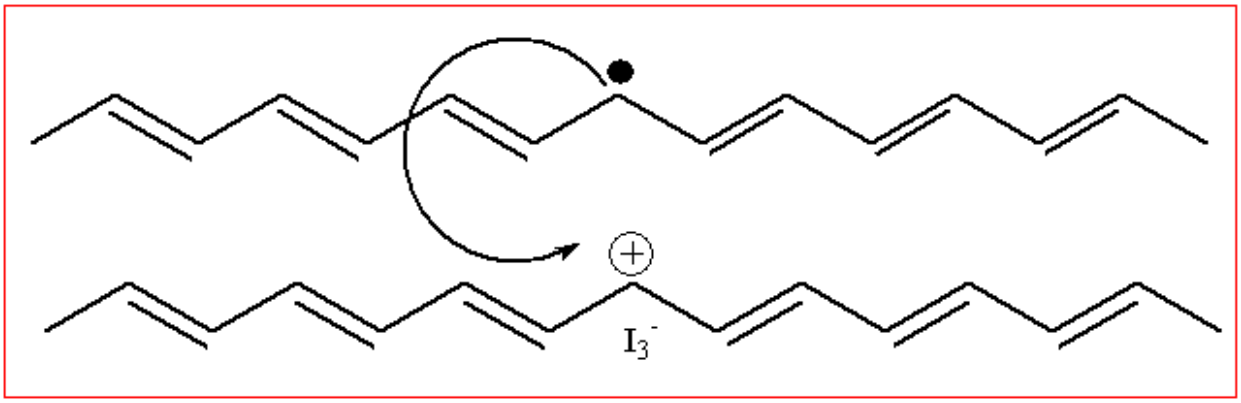

Figure 2.9. Intersoliton hopping in trans-polyacetylene.

The charged solitons are trapped by the dopant ions and neutral solitons are free to move. When neutral soliton passes close by a charged soliton, an electron can hop between the mid gap states belonging to the solitons [28].

2.2. Polymer Electrolytes

After P.V. Wright's discovery of ionic conductivity in alkali metal salt complexes of poly(ethylene oxide) (PEO) in 1973 [29], polymer electrolytes were proposed for batteries in 1978 because they combine the advantages of solid state electrochemistry with the ease of processing inherent to plastic materials [30].

Polymer electrolytes are solid solutions of alkali metal salts in polymers (not to be mixed up with polyelectrolytes, in which either the cation or the anion is covalently fixed to the polymer repeat unit). The interest in these solid-state ionic conductors comes from the possibility of using them to substitute the liquid electrolytes in several electrochemical devices. The major challenge in replacing the liquid or gel electrolyte by polymeric one is to keep the high operation efficiency, similar to the electrochemical devices based on liquid junction. Besides improving the stability of the active interfaces, allowing a long-term durability, polymer electrolyte eliminates problems concerning evaporation or leakage of the solvent.

Poly(ethylene oxide), PEO is the reference polymer for ionic conduction, since it is best for alkali salts because of the high Lewis base character of the oxygen atoms present in it. Due to this reason, greater efforts have been devoted to make polymer electrolytes based on, PEO, combining it with several salts [30].

Initially it was assumed that the crystalline domains are responsible for ion transport, with the ion moving along the PEO helices as the primary mechanism; however it was soon established that the amorphous phase alone gives rise to high ion transport [31].

Random copolymers with fully amorphous morphology are obtained by interspersing ethylene oxide with methylene oxide units [32]. The methylene oxide units break up the regular helical pattern of PEO, and in doing so suppresses crystallization. Both the host polymers and the electrolytes derived from them are amorphous; sometimes they are referred to as amorphous PEO (a-PEO). Electrolytes based on a-PEO generally have conductivities around 10^{-4} S/cm [33] at ambient temperature. Similarly, dimethyl siloxy units have been introduced between medium length PEO units to produce an amorphous polymer, dimethyl siloxy linked PEO.

The polymer electrolyte used in this study is amorphous poly(ethylene oxide), POMOE, with a repeating unit of $CH_2O(CH_2CH_2O)_9$. It is known to have very good ionic conductivity at room temperature [33]. The redox couple used to complex with the polymer electrolyte is iodide/triiodide.

2.3 Photovoltaic Energy Conversion Using Conducting Polymer

In photovoltaic energy conversion, the solar cell converts light energy directly into electrical energy. The materials, which are used for this purpose, are classified as semiconductors. A tremendous research and development was made in enhancing efficiency and practical application of solar cells using inorganic semiconductor materials such as silicon, gallium arsenide, and sulfide salts of cadmium and copper, and other alloys of these materials.

Research work on polycrystalline and amorphous silicon is still active. Moreover, organic semiconductors and conjugated polymers have been also used in solar cell devices. The similarity of their electrical and optical properties to the inorganic semiconductors makes the polymers an alternative for electronic and optoelectronic devices. Polymeric materials can be considered as n-type and p-type semiconductors. Thus, in the use of these materials for solar cell devices, Schottky barrier theory as developed for inorganic semiconductors can be applied to them.

As far as inorganic semiconductor is concerned the most popular junction in electronic industry is the p-n junction. Most of the organic diodes are based on another structure, the metal-semiconductor or Schottky barrier junction. Although it is possible to construct the p-n junction of organic diodes, it is not stable yet. The main source of the instability of a p-n organic diode is the great ability of doping impurities diffuse from the p-to-n side and vice versa [34]. Photovoltaic effect in the rectifying Schottky junction can be explained as follows. The absorption of photon energy greater than the band gap results in the generation of electron-hole pairs or the absorption of a photon creates an exciton rather than free charge carriers [35]. The photovoltaic current in the cell is then a direct transport of the free carriers in the first case while in the second case, in order to generate photocurrents, the excitons must dissociate into electrons and holes either in the bulk of the organic polymer or metal-polymer interfaces.

In general the sequence that leads to a photovoltaic effect in organic polymer solar cell device can be described by simple four steps as follows [35, 36]: photogeneration of charges, charge separation, charge transport and charge collection to yield current.

2.4. Photoelectrochemical Solar Energy Conversion

2.4.1. Photoelectrochemical effects

A photoelectrochemical effect is defined as the production of a change in redox potential or current in an electrode/electrolyte system as a result of irradiation. The effect is caused by either a photoelectrochemical reaction producing electroative products in the bulk solution or the presence of a photosensitive electrode. Solar irradiation produces photoelectrochemical effects on most, not all, surfaces. Photoelectrochemical effects at clean metal electrodes are very small. Semiconductors on the other hand have been found to produce pronounced photoelectrochemical effects [37].

Photoelectrochemical solar energy conversion is based on the junction between a semiconductor and an electrolyte. A typical photoelectrochemical cell (PEC) is shown in Figure 2.10. It consists of a semiconductor electrode, a counter electrode, and an electrolyte containing a redox couple. The PECs that convert light into electricity are termed "electrochemical photovoltaic" or "regenerative cells" and those that generate chemical fuels are "photoelectrosynthetic" or "non-regenerative cells".

An illuminated PEC bears a formal resemblance to a traditional schottky barrier photovoltaic device, with metal layer connecting the semiconductor replaced by an electrolyte containing adequate redox couple. In contrast to solid conventional semiconductor solar cells, PEC solar cell uses liquid electrolyte or ion-conducting solid phase as charge transport medium.

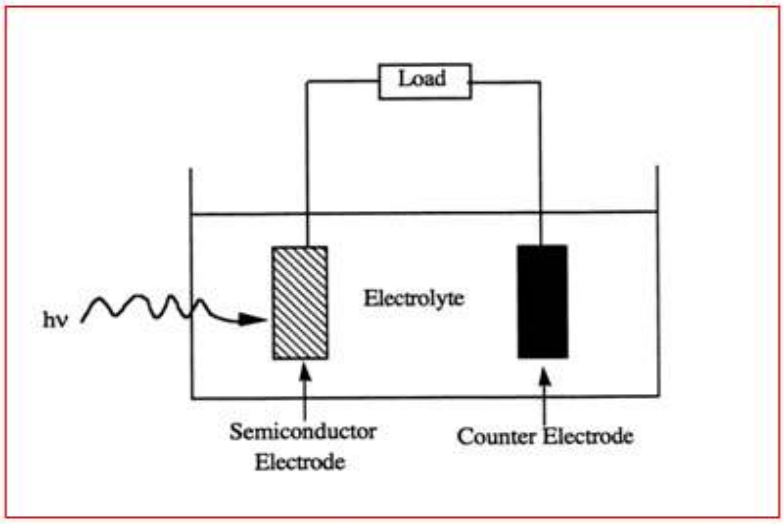

Figure 2.10. Photoelectrochemical cell

2.4.2 Semiconductor-Electrolyte Interfaces

It is more difficult to describe quantitatively the energetics of a semiconductor/electrolyte contacts. Generally the solvent and electrolyte do not rapidly accept or donate charges to the semiconductor.

Instead donor/acceptor pair, the redox couple, is deliberately dissolved in the liquid phase. The dissolved redox couple provides the chemical species that can rapidly exchange charges with the solid.

The redox couple also controls the Fermi level of the liquid phase. In this notation, if A is the oxidized form of the redox couple, and A^- is the reduced form of the redox system then the electrochemical potential of the electrolyte is given by the Nernst equation:

$$E=E^{o}(A/A^{-})+(RT/nF)\ln\{[A]/[A^{-}]\} \quad (4)$$

E^{o} (A/A^{-}) describes the electrochemical potential of the redox pair A/A^{-} under standard state condition. The second term in equation (4) is a statistical factor that accounts for any difference in the concentration of the redox species between the standard state and the actual solution of interest.

To obtain a qualitative prediction of the interfacial charge flux, the Fermi level of the solution must be located relative to Fermi level of the semiconductor. However, Nernst potentials in liquids, E (A/A^-), are generally referenced to standard redox potential, because it is impossible to obtain an absolute value for the energy of an isolated redox solution [38]. The normal hydrogen electrode (NHE) consisting of Pt electrode in contact with 1M H^+ (aq)/1.0 atm H_2 (g), is the most common referenced potential. Theoretical estimates have placed the energy of NHE at 4.4 to 4.7eV versus vacuum level [38].

The important energetic trends for a series of different liquid contacts can be determined by measurement of the solution redox potential relative to standard reference electrode. Within this model, solutions with more positive redox potentials should induce greater charge transfer in contact with n-type semiconductors, but should induce less charge transfer in contact with p-type semiconductors. For an n-type semiconductor, a scheme of the energetics of the interface before and after contact is shown in Figure 2.11.

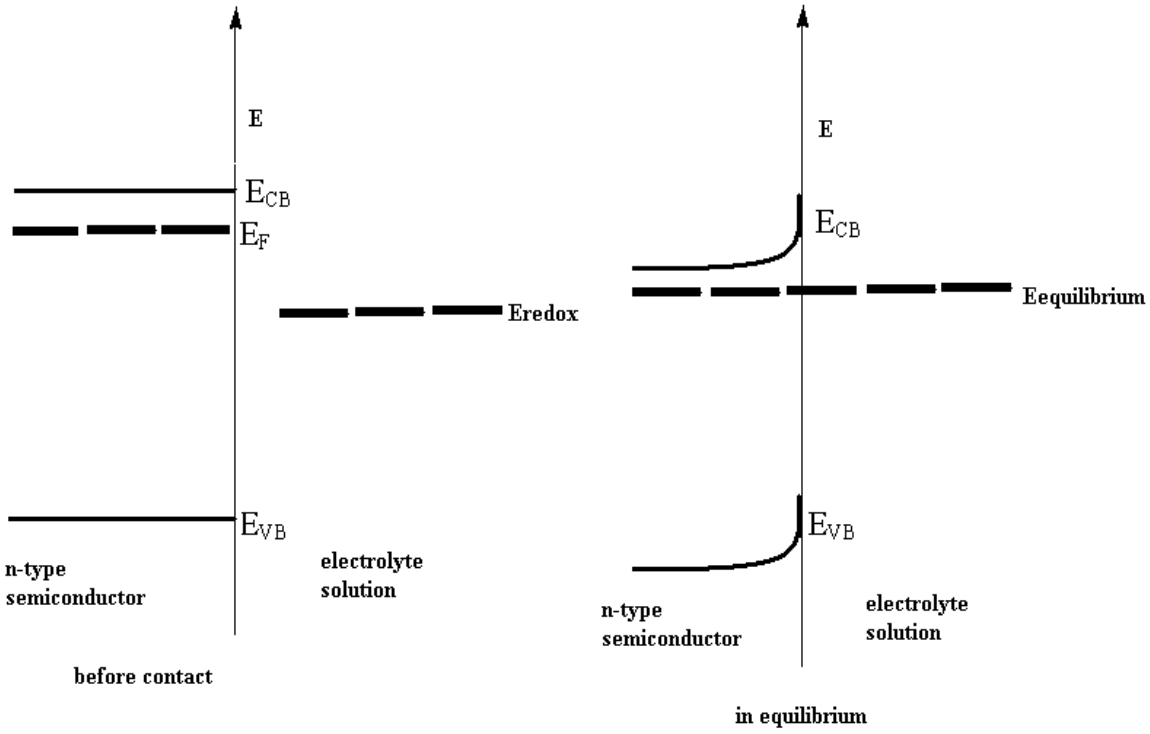

Figure 2.11. Energetics of an n-type semiconductor-electrolyte solution interface, before contact and at equilibrium.

After contact, the former different redox potential E_{redox} of the electrolyte solution and the Fermi level E_F of the semiconductor equilibrate. As a result, the interface gets charged, which leads to a bending of the valence band (VB) and the conduction band (CB) of the semiconductor. Due to illumination of the semiconductor electrons may be excited, jumping from the valence band to the conduction band.

In the space charge layer the generated charges are now separated, because the holes are attracted towards the interface and the electrons to the opposite direction. As a result, a current is observed in an outer circuit.

For a p-type semiconductor the situation is reversed. Valence and conduction bands are now bent downwards, and consequently the electrons excited by illumination are attracted by the interface, pushing the holes away. The current flowing through an outer circuit has now opposite sign. A scheme of the situation in a p-type semiconductor is shown in Figure 2.12.

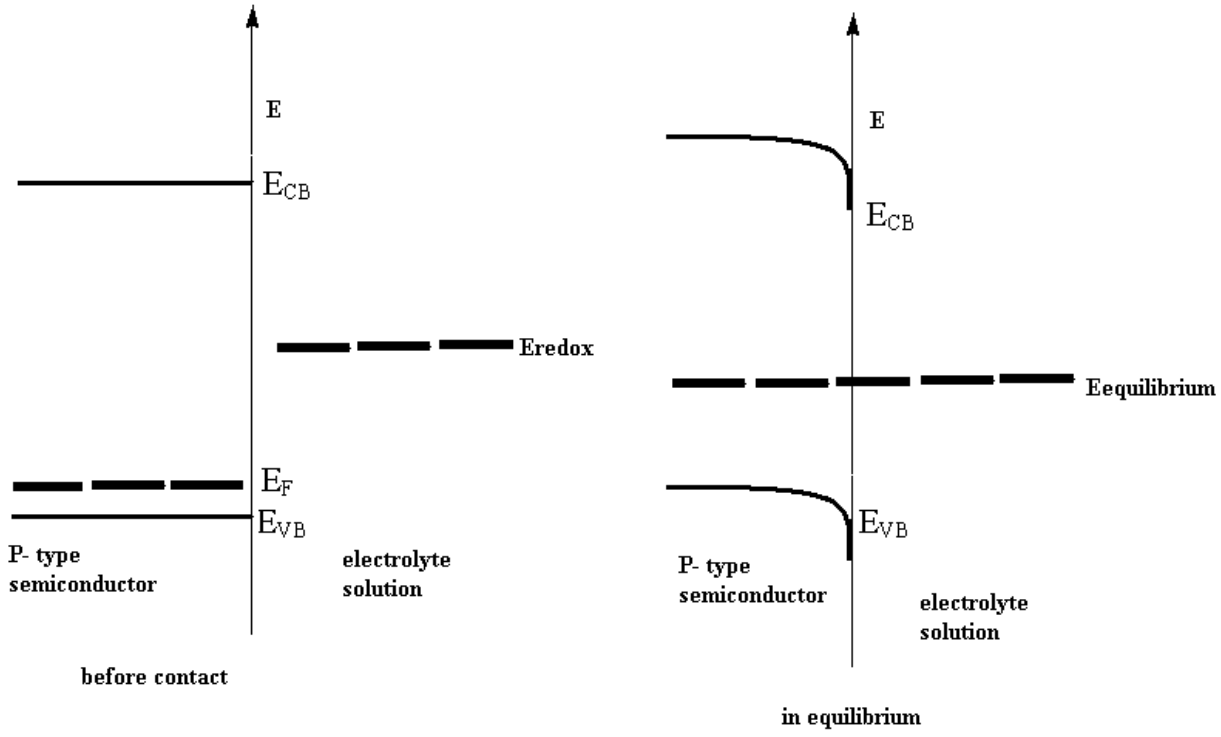

Figure 2.12. Energetics of a p-type semiconductor-electrolyte solution interface, before contact and at equilibrium.

2.5. Solar Cell Parameters

In solar cells the photon energy is converted into electrical energy. When a sheet of solar cell material is exposed to sunlight, a photon with energy greater than or equal to the band gap energy, E_g, of the semiconductor is absorbed in the cell thereby generating photocurrent. On the other hand, photon energy less than E_g makes no contribution to the cell output. The incident photon energy depends on the wavelength of the light and hence the band gap energy, E_g, is related to the wavelength.

To derive the solar cell output parameters that are used for characterization of photoelectrochemical properties of the device; we shall consider an ideal Schottky diode. When the cell is illuminated, the total current density, I, is equal to the sum of the photocurrent density, I_{ph}, and the dark current density, I_{dark}.

$$I = I_{ph}\text{-}I_{dark} \tag{5}$$

The dark current-voltage characteristics of the solar cell is expressed as

$$I = Io[\exp\left(\frac{qV}{nKT}\right)] \tag{6}$$

Where I is the total current density (dark current density), I_o is the inverse saturation current density which is the current density flowing under sufficiently high reverse bias, q is the charge on an electron, V is the applied voltage, n is the ideality factor of the diode (for an ideal diode n = 1), k is the Boltzmann constant and T is the absolute temperature.

Thus the I-V characteristics of the Schottky diodes under illumination is given by

$$I = Iph - Io[\exp\left(\frac{qV}{nKT}\right)] \tag{7}$$

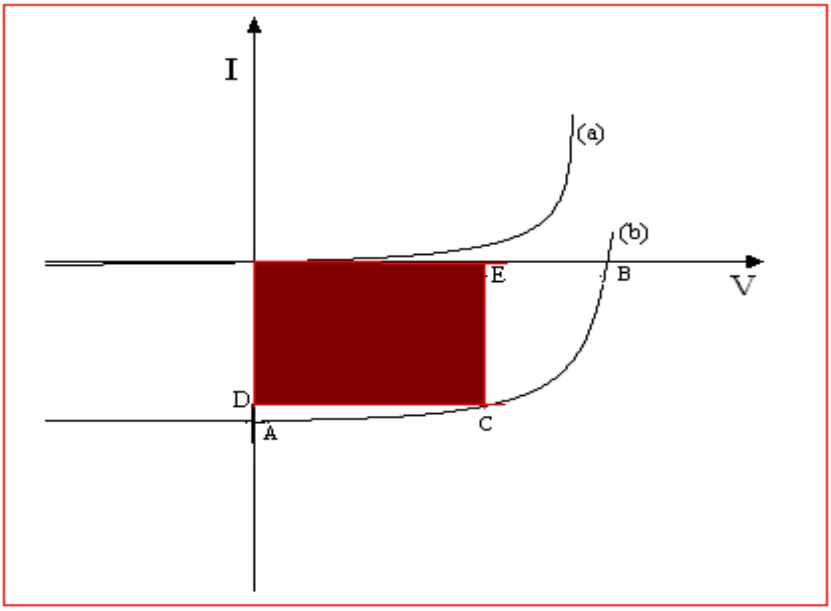

Figure 2.13. Typical current-voltage characteristics of Schottky diodes (a) in the dark (b) under illumination

Short circuit current (I_{sc})

This is the current that flows through an illuminated solar cell when there is no external resistance (i.e., when the electrodes are simply connected or short-circuited). The short-circuit current is the maximum current that a device is able to produce. Under an external load, the current will always be less than I_{sc}.

Open circuit voltage (V_{oc})

It is the maximum voltage attainable in a solar energy conversion device. The cell is placed in an open-circuit and illuminated. Electrons and holes separate and flow towards the low and high work function materials, respectively. At some point the charge build-up will reach a maximum equal to the V_{oc}. At open-circuit voltage, the net current, I, is zero. Therefore using Equation (7), the V_{oc} is given by Equation (8)

$$\mathrm{Voc} = \frac{nKT}{q}\left(\ln\frac{\mathrm{Iph}}{\mathrm{Io}} + 1\right) \tag{8}$$

Fill factor (FF)

The ratio of a photovoltaic cell's actual maximum power output to its theoretical power output if both current and voltage were at their maxima, I_{sc} and V_{oc}, respectively. This is a key quantity used to measure cell performance. It is a measure of the squareness of the I–V curve. The formula for FF in terms of the above quantities is:

$$\mathrm{FF} = \frac{I_{max}\, V_{max}}{I_{sc}\, V_{oc}} \tag{9}$$

Power Conversion Efficiency (η)

The ratio of power output to power input. In other words, PCE measures the amount of power produced by a solar cell relative to the power available in the incident solar radiation (P_{in}). P_{in} here is the sum over all wavelengths and is generally fixed at 100 mW/cm^2 when solar simulators are used. This is the most general way to define efficiency.

$$\eta\% = \frac{P_{max}}{P_{in}}\frac{FFI_{sc}V_{oc}}{P_{in}} \tag{10}$$

Incident monochromatic photon to current conversion efficiency (IPCE)

Incident monochromatic photon-to-current conversion efficiency also called external quantum efficiency is defined as the ratio of the number of collected charge carriers to the number of incident photons at the device. It is given by the equation:

$$IPCE\% = \frac{1240I_{sc}}{\lambda P_{in}} \tag{11}$$

Where I_{sc} is short circuit current ($\mu A /cm^2$), λ the excitation wavelength (nm) and P_{in} the incident photon intensity (W/m^2). Light of different wavelength is absorbed at different depths of the photoactive electrode.

2.6. Factors affecting the efficiency of an organic solar cell

Power conversion efficiency of solar cells is directly correlated to the three key parameters, namely I_{sc}, V_{oc}, and FF. This means η is inherently related to material properties, device structure and interface effects. The I_{sc} of polymer solar cells is affected by several factors including generation and dissociation rates of excited states, as well as the mobility of free charge carriers.

The method of blending conjugated polymers with high electron affinity molecules, such as C_{60} and its derivatives, has become the most efficient and rapid exciton dissociation method resulting in solar cells with high power conversion efficiencies.

To enhance the optical absorption in solar cell materials two mechanisms can be suggested, namely utilizing thick films and/or harvesting photons in the red and near infrared portion of the solar spectrum. The first option is practically limited by the low charge carrier mobility and lifetime.

The disordered nature of polymer chains forbid formation of perfect electronic wave function overlaps, which in the case of inorganic materials leads to band transport. Instead, charge carriers are highly localized and their transport is limited by the degree of the spatial and energetic disorder. Consequently, the mobility of charge carriers, in most conjugated polymers, is quite low, typically 10^{-3} to 10^{-6} cm^2/Vs [39]. As a consequence, in thick films, most of the photogenerated carriers disappear through recombination processes or forms space charges that limit flow of current. The second option, utilizing long wavelength photons, can be realized by using low band gap polymers [39].

The second photovoltaic parameter that limits efficiency is the open-circuit voltage. In general, V_{oc} is limited by several factors including interfacial energy levels, shunt losses, interfacial dipoles and morphology of the active film.

For donor/acceptor based solar cells with Ohmic contacts, V_{oc} is mainly determined by the difference between the HOMO of the donor polymer and the LUMO of the acceptor molecule indicating how much the electronic levels are crucial in determining the efficiency of such solar cells.

The third important parameter that limits efficiency is a fill factor. The direct relation of FF with current density indicates that it is greatly affected by the mobility of the charge carriers. Moreover, series resistance is also one of the limiting factors as observed in organic bilayers as well as in donor/acceptor-based solar cells [39].

3. EXPERIMENTAL METHODS

3.1 Materials

In this study the conjugated semiconducting polymers used as photoactive electrodes are mixture of (MEH-PPV) (Aldrich) and (MDMO-PPV) (Aldrich) and pure MEH-PPV (Aldrich). The polymer electrolyte used is amorphous poly(ethylene oxide), from the poly[oxymethylene-oligo(oxyethylene)] (POMOE) family, with a repeating unit of $CH_2O(CH_2CH_2O)_9$. The redox couple used to complex with the polymer electrolyte is iodide/triiodide. The counter electrode used is ITO-glass coated with oxidized poly(3,4-ethylenedioxythiophene), PEDOT. The chemical structures of the substances used in this work are depicted in Figure 3.1.

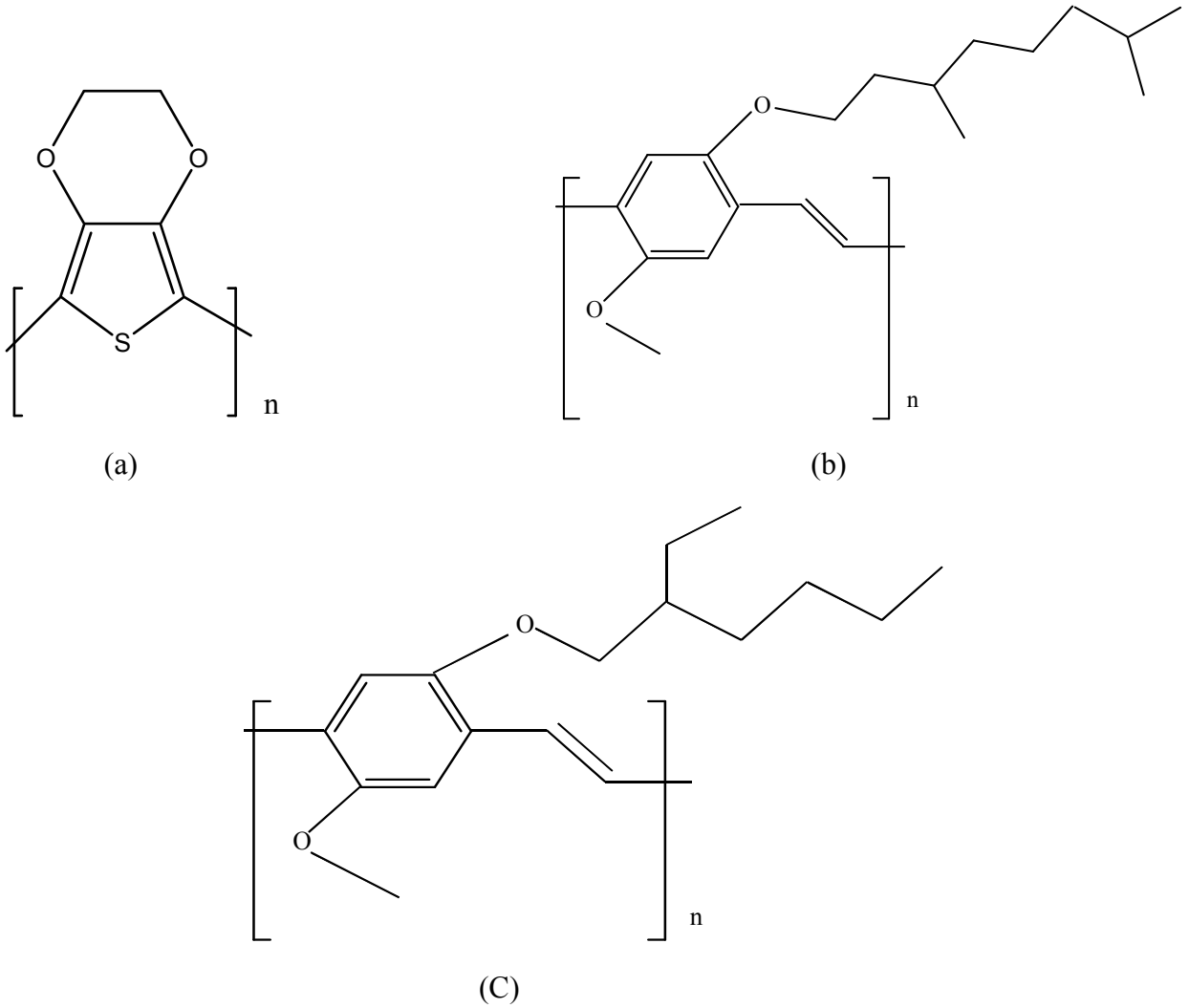

Figure 3.1. The chemical structure of substances used in this work (a) PEDOT (b) MDMO-PPV and (c) MEH-PPV

3.2 Experimental Set-Up

A schematic of the experimental set-up used to measure the photoelectrochemical properties of the device is shown in Figure 3.2. A 250 W tungsten-halogen lamp regulated by an Oriel power supply (Model 66182) is used to illuminate the PEC. The resulting photoelectrochemical properties were studied using CHI630 electrochemical Analyzer. The white light intensity was measured in the position of the sample cell with a Gigahertez-optik optometer with RW-37; single channel radiometric and photometric detector heads (Model X1-1). For intensity dependence measurements a series of neutral density filters were placed between the light source and the sample holder to vary the light intensity incident on the sample. Optical absorption measurements were carried out using Spectroscopic GENSEYS 2PC UV/VIS spectrometer. A grating monochromator (Model 77250) was used to select a wavelength manually between 300 nm and 800 nm at an interval of 10 nm. The spectra were corrected for the spectral response of the lamp and the monochromator by normalization to the response of a calibrated Silicon photodiode (Hamamatsu, model S-1336-8BK).

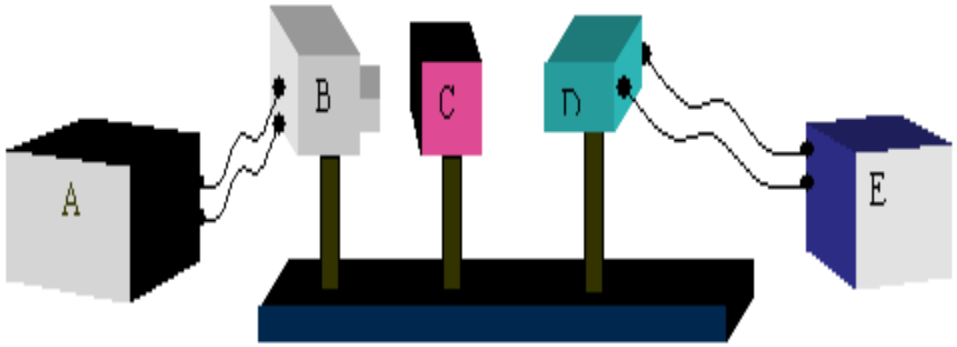

Figure 3.2. General experimental set-up for the photoelectrochemical measurements [40].

(A) power supply (B) lamp housing (C) monochromator
(D) sample holder and (E) an output measuring apparatus

3.3 Procedures

3.3.1 ITO-Coated Glass Preparation

ITO-coated glass of area 3.75 cm^2 was cleaned successively with acetone, iso-propanol, ethanol and deionized water.

3.3.2 Solution Preparation

48.47 mg of KI, 7.41 mg of I_2 and 311 mg of POMOE were dissolved separately in 25 ml of methanol. The mole ratio of I_2 was 1/10 to that of KI. The ion concentration, as given by the ratio of oxygen atoms in the POMOE to the K^+ ion, taking into account both oxymethylene and oxyethylene oxygen atoms was 25. The triodide (I_3^-) ion is formed by mixing iodide (I^-) from KI with I_2. Equal volumes of these three solutions were mixed, where the polymer was complexed with I_3^-/I^- redox couple. A 0.1 M solution of EDOT was prepared in 0.1 M LiClO4- acetonitrile. A mixture of 2.5 mg MEH-PPV and 2.5 mg of MDMO-PPV and 2.5 mg of pure MEH-PPV was dissolved in 1 ml 1, 2-dichlorobenzene solution separately to prepare the photoactive electrodes.

3.3.3 Electrode Preparation

The quasi Ag/AgCl reference electrode was prepared by applying a potential of 4.60 V from a dc power source between silver and platinum wires that were immersed in a saturated Potassium chloride solution. Photoactive electrodes were formed by drop casting solutions of mixture of MEH-PPV and MDMO-PPV and pure MEH-PPV on pre-cleaned ITO coated glass substrates separately. After drying in air, the polymer films at the edge were cleaned with 1, 2-dichlorobenzene for an electrical contact area. The slow evaporation of the solvent at room temperature resulted in the formation of uniform films.

The polymer PEDOT film was prepared by the electrochemical oxidation of the monomer EDOT in a three-electrode one-compartment electrochemical cell with platinum foil counter electrode, quasi Ag/AgCl reference electrode and ITO-coated glass working electrode. The solution used for the polymerization contained 0.1 M EDOT in 0.1 M $LiClO_4$-acetonitrile.

The polymerization was carried potentiostatically at 2.0 V versus Ag/AgCl quasi reference electrode for three seconds, at which potential the ITO-coated glass surface was covered with light blue PEDOT. The oxidized form of the polymer was rinsed with acetonitrile and dried in air. The film formed was semi-transparent. PEDOT improves the charge transfer between the ITO and the I_3^-/I^- redox couple [41]. It is chosen as a counter electrode, because it is less costly and can easily be prepared electrochemically to a desired transparency [41].

3.3.4 Construction and Structures of Devices

A solid-state PEC constructed in this study contained films of mixture of MEH-PPV and MDMO-PPV and pure MEH-PPV coated on ITO-coated glass light harvesting unit, POMOE solid electrolyte complexed with I_3^-/I^- redox couple and a conducting PEDOT coated on ITO counter electrode. The POMOE complexed with an I_3^-/I^- was deposited on the top of the photoactive films by solvent casting from methanol solution and dried in air at room temperature. The construction of the cell was finalized by pressing together the photoactive electrode covered with electrolyte film and the PEDOT counter electrode. The devices were then mounted in a sample holder inside a metal box having a 1 cm x 1 cm light entrance window, which determined the illumination area. The basic device structure of solid-state PEC used in this study is shown in Figure 3.3.

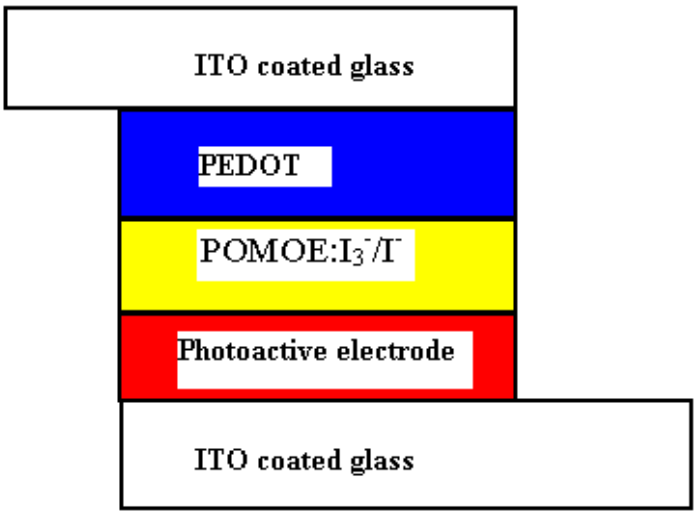

Figure 3.3. Basic device structure of solid-state PECs used in this study

4. Results and Discussion

4.1. Current-Voltage Characteristics

Figure 4.1, and 4.2 respectively, shows the current-voltage curves for ITO │ (MEH-PPV:MDMO-PPV) │POMOE:I_3^-/I^-│PEDOT│ITO and the same for MEH-PPV, based PECs, in the dark and under white light illumination with incident light intensity of 100 mW/cm^2 from the front side, (PEDOT│ITO) side. The photoelectrochemical characteristics of the devices are compared in Table 1.

In the dark, the current for both devices was negligible and remained relatively constant in the negative potential range while a larger anodic current was observed in the larger positive potential range. The positive applied potential acts to diminish the effects of the internal barrier field that is set at the polymer/electrolyte junction. As a result, charge carriers acquire enough energy to cross the barrier, resulting with large anodic currents. On the other hand, applying a negative potential enhances the barrier potential and only a small current flows. The current response of the devices to the applied potentials in the dark indicates that the devices exhibit the desirable photoelectrochemical properties. Under illumination, cathodic photocurrents were observed in both MEH-PPV [42] and MEH-PPV:MDMO-PPV based PECs having better I_{sc} and V_{oc} for PEC in which photoactive electrode is mixture of MEH-PPV and MDMO-PPV. This is because the better absorption spectrum of the mixed polymer. This leads to produce high amount of charge carriers. The optical absorption spectra of each polymer and mixture of the two are shown in Figure 4.3.

The holes generated during illumination go to the back electrode (cathode). At the PEDOT│ITO (anode), the iodide generated at the cathode is oxidized to triiodide. Since there is one redox couple, the process is cyclic and therefore there is no net chemical reaction; the PECs converts light to electricity operating in regenerative mode.

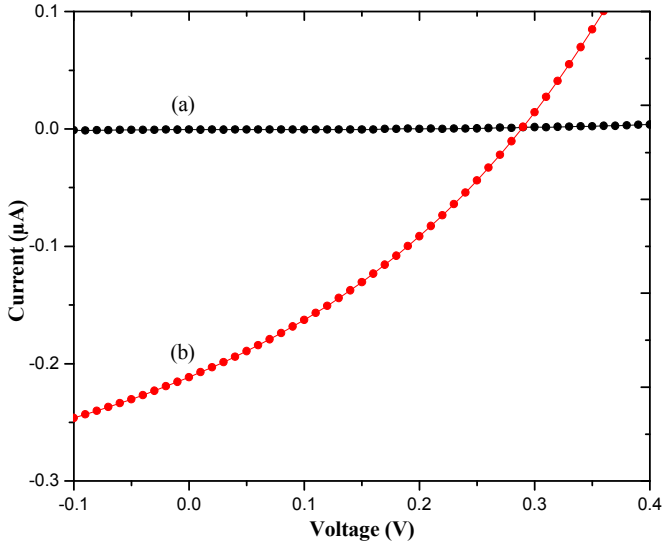

Figure 4.1. Current-voltage characteristics of ITO │(MEH-PPV:MDMO-PPV)│POMOE:I_3^-/I │PEDOT│ITO PEC (a) in the dark and (b) under illumination through front side with light intensity of 100 mW/cm^2.

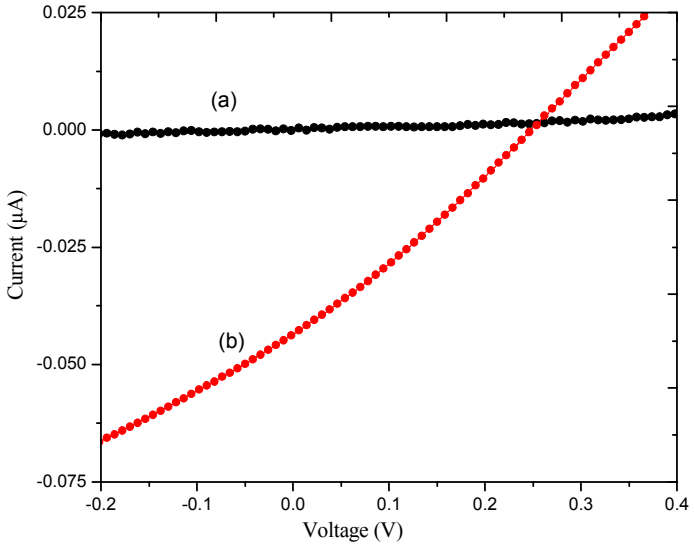

Figure 4.2. Current-voltage characteristics of ITO│MEH-PPV │POMOE:I_3^-/I^-│PEDOT│ITO PEC (a) in the dark and (b) under illumination through front side with light intensity of 100 mW/cm^2.

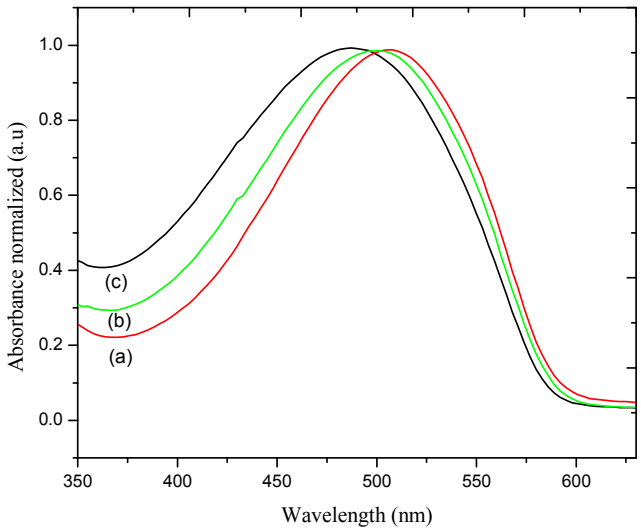

Figure 4.3. Normalized optical absorption spectra of (a) MEH-PPV (b) mixture of MEH-PPV and MDMO-PPV and (c) MDMO-PPV

Table 1. The typical photoelectrochemical properties have been calculated from the analysis of the I-V characteristics for the solid state PECs under 100 mW/cm^2 illumination.

Photoactive electrode	**V_{oc} (mV)**	**I_{sc} (µA)**	**V_{max} (mV)**	**I_{max} (µA)**	**FF**	**Ref.**
Mixture of MDMO-PPV and MEH-PPV	289.7	0.21	166.53	0.118	0.32	-
MEH-PPV	310	0.14	-	-	0.30	[42]

4.2 Transient Properties of I_{sc} and V_{oc}

4.2.1 Transient Property of I_{sc}

The transient study of short circuit current was measured for mixture of the two polymers and pure MEH-PPV. The I_{sc} induced by the periodical blocking of the light path to the sample from the front, PEDOT │ITO side, for mixture of MEH-PPV and MDMO-PPV and pure MEH-PPV PECs is shown in Figure 4.4. In both cases very small current is observed before the light is switched on. When switching on the light, the current will increases steadily as a function of time. A decrease in photocurrent was observed, however, insignificant (the reason for the decrease may be due to a small capacitive photocurrent) and then stable at 0.21μA/cm^2 for the mixed and 0.0265 μA/cm^2 for pure MEH-PPV based PEC. When the light turned off, the current decayed abruptly.

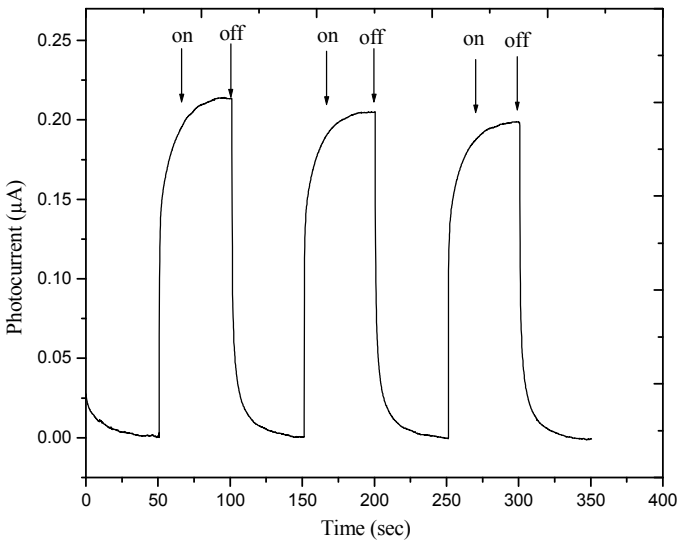

(a)

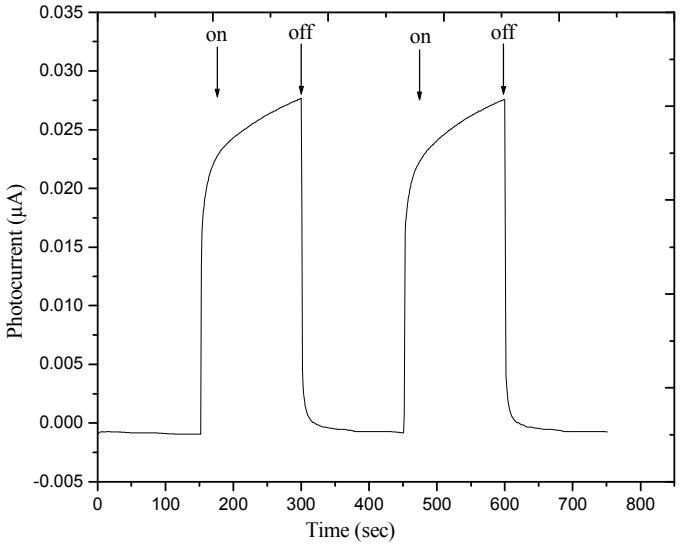

(b)

Figure 4.4. I_{sc} change during switching light on and off for (a) ITO│(MEH-PPV:MDMO-PPV)│POMOE:I_3^-/I^- │PEDOT│ ITO and (b) ITO│MEH-PPV│POMOE:I_3^-/I^- /PEDOT│ ITO based PECs at 100 mW/cm^2.

4.2.2 Transient Property of V_{oc}

Illumination of PECs based on a mixture of MEH-PPV and MDMO-PPV and pure MEH-PPV resulted in an immediate increase in a photovoltage to the steady state value of 220 mV, and 130 mV respectively, which remained constant until the light was blocked. As the light was blocked, the photovoltage slowly decayed to zero for the mixed polymer and 30 mV dark potential for pure MEH-PPV based PEC shown in Figure 4.5.

As can be seen from the Figures, (Figure 4.4 and 4.5), only the I_{sc} value of PEC based on a mixture of MEH-PPV and MDMO-PPV is consistent with the value in the I-V curve. Table 2 summarizes the comparison between values obtained using I-V and transient studies.

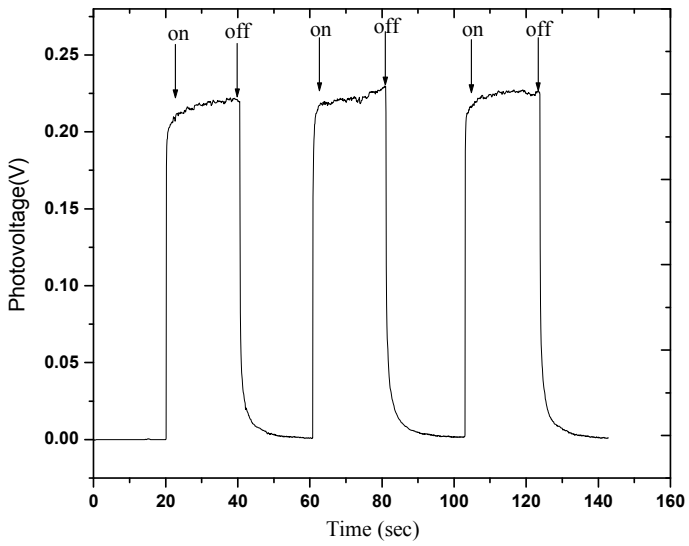

(a)

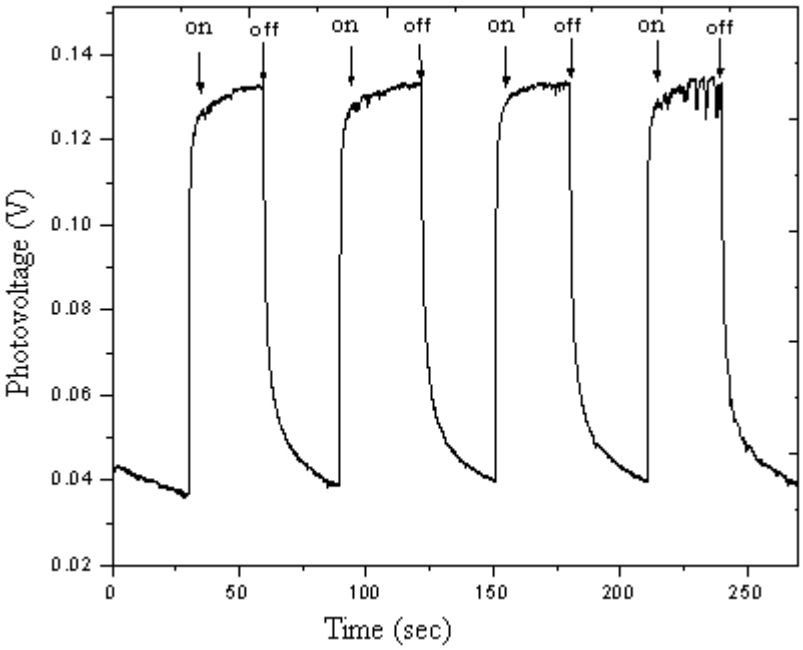

(b)

Figure 4.5. V_{oc} change during switching light on and off for (a) ITO |(MEH-PPV:MDMO-PPV)|POMOE:I_3^-/I^-|PEDOT|ITO and (b) ITO|(MEH-PPV)|POMOE:I_3^-/I^-|PEDOT|ITO based PECs at 100 mW/cm^2

Table 2. Comparison between values obtained using I-V and transient studies

Photoactive electrode	**I-V**		**Transient study**	
	V_{oc} (mV)	**I_{sc} (μA)**	**V_{oc} (mV)**	**I_{sc} (μA)**
MEH-PPV:MDMO-PPV	289.7	0.21	220	0.21
MEH-PPV	251.08	0.0437	130	0.0265

4.3 Spectral Response

The photocurrent action spectra plotted in terms of IPCE% versus wavelength illuminated from (a) front side and (b) backside for the solid-state PEC based on a mixture of MEH-PPV and MDMO-PPV is shown in Figure 4.6. The IPCE% obtained at the maximum absorption (490 nm) for the solid-state PEC was 0.0034 % and 0.00013 % for the front side and backside illumination, respectively. Comparison of the front side and backside monocromatic conversion efficiencies showed that the front side illumination was greater than that of the backside illumination at the maximum absorbance. The reason behind this difference is the optical filtering effect of the conjugated polymer films.

When light is illuminated from the backside, only small fraction of the excitons produced by light absorption reached the interface to dissociate into carriers. However, at lower wavelengths, the IPCE% from the backside illumination was greater than that from the front side. This is because at lower wavelength, light penetrates deeper and the exciton will be created much closer to the photoactive electrode/redox couple interface so that relatively large photocurrent will be measured.

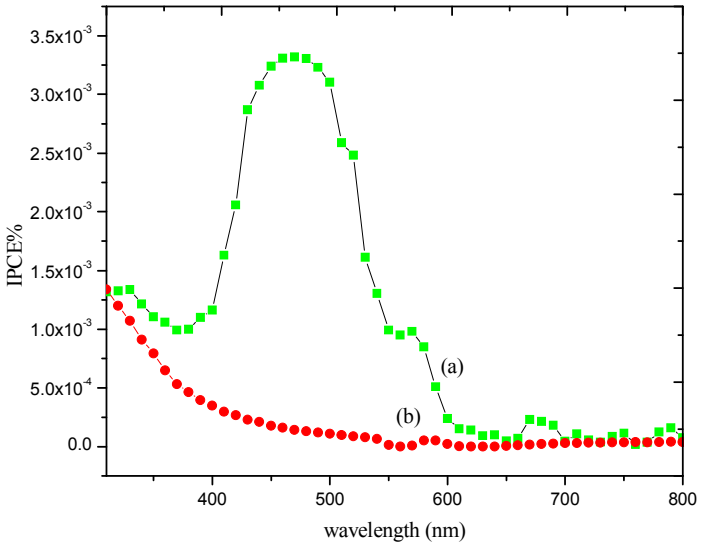

Figure 4.6. Photocurrent action spectra illuminated from the (a) front side and (b) backside of ITO │(MEH-PPV:MDMO-PPV) │POMOE:I_3^-/I^-│ PEDOT │ITO PEC with monochromatic light.

The normalized optical absorption spectra of the mixture and the normalized photocurrent action spectrum of the solid-state PEC based on MEH-PPV: MDMO-PPV illuminated from front and backside is shown in Figure 4.7. Since illumination through the front side of the cell produces a spectral response, which is resembles to the optical absorption spectrum of the polymer mixture, then the electrolyte/conducting polymer junction is responsible for the photovoltaic behavior.

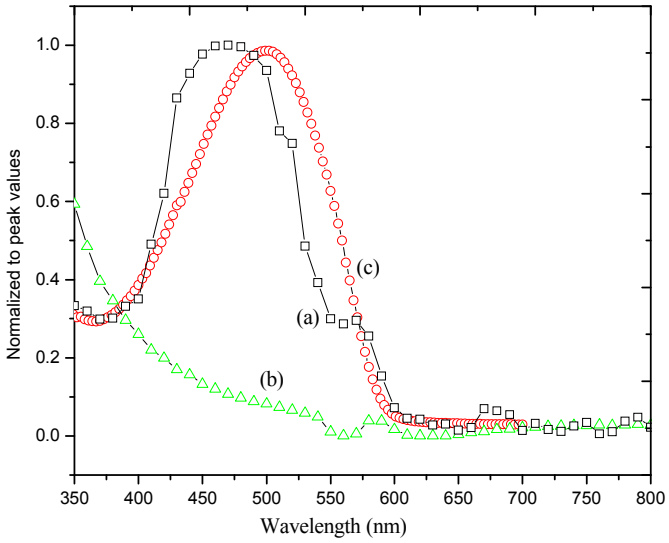

Figure 4.7. Normalized photocurrent action spectra illuminated from (a) front side and (b) back side of ITO│(MEH-PPV:MDMO-PPV) │ POMOE:I_3^-/I^-│ PEDOT│ITO PEC and (c) normalized optical absorption spectra of mixture of MEH-PPV and MDMO-PPV

4.4 Dependence of I_{sc} and V_{oc} on Incident Light Intensity

4.4.1 Dependence of I_{sc} on incident light intensity

The variation of the I_{sc} with light intensity for the solid-state PEC is shown in Figure 4.6. The I_{sc} of the PEC increased with increasing light intensity and was proportional to P_i^{α}, where α a power factor and P_i is the incident light intensity. Therefore, the plot of $\log I_{sc}$ versus $\log P_i$ yielded straight line with α is equal to 0.793 and 0.60 for the solid-state PECs based on a mixture of MEH-PPV and MDMO-PPV and pure MEH-PPV respectively [42]. The higher value of α for PEC having MEH-PPV:MDMO-PPV as photoactive electrode is because of the fact that the less exciton recombination due to surface states that act as recombination centers [43].

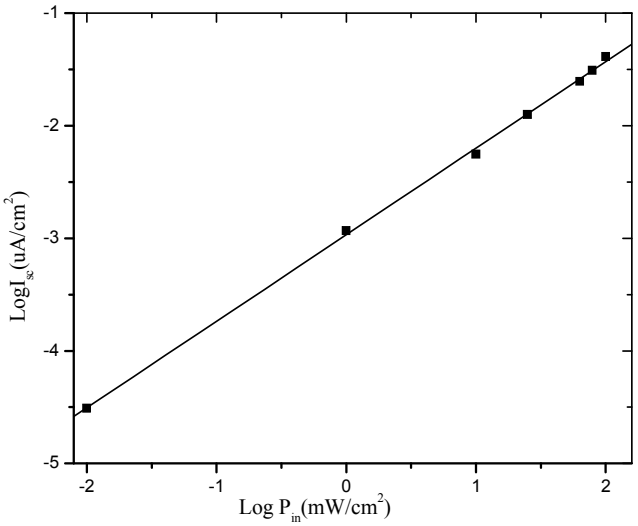

Figure 4.8. Light intensity dependence of I_{SC} of ITO│MEH-PPV:MDMO-PPV│POMOE:I_3^-/I^- │PEDOT│ITO

4.4.2 Dependence of V_{oc} on incident light intensity

For Schottky junction solar cells under open-circuit conditions, no net current will flow through the junction. Thus, Eq. (8) can be rearranged to yield the following relationship:

$$V_{oc} = \frac{nKT}{q}\left(\ln \frac{Iph}{Io}\right) \qquad \text{for } I_{ph} \gg I_o$$

As can be seen from Equation (8), V_{oc} increases logarithmically with the light intensity because I_{ph} is linearly proportional to the incident light intensity. The plot of V_{oc} versus log P_{in} of the ITO| MEH-PPV:MDMO-PPV| POMOE: I_3^-/I^-| PEDOT| ITO solid-state PEC is shown in Figure 4.9. V_{oc} increases logarithmically with the light intensity, in agreement with the projected behaviour of Schottky barrier solar cells.

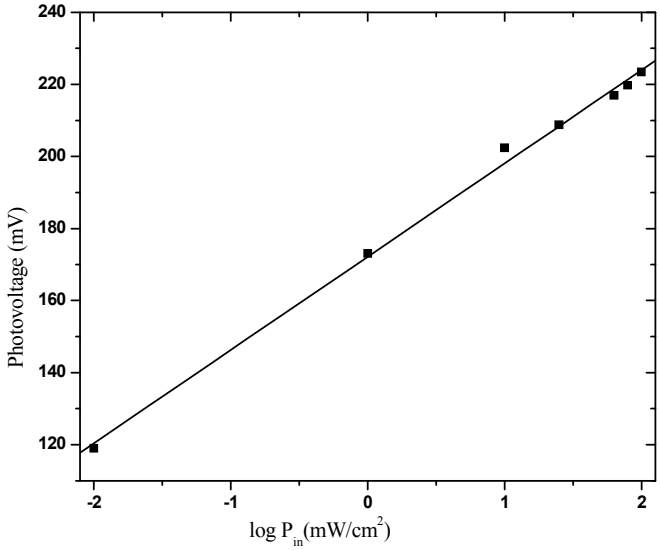

Figure 4.9. Light intensity dependence of V_{OC} of ITO │MEH-PPV:MDMO-PPV │POMOE:I_3^-/I^- │PEDOT │ITO

5. Conclusions

In this study it has been shown that the optical energy is converted into electrical with a mixture of MEH-PPV and MDMO-PPV photoactive electrode based solid state PEC. The optical absorption spectrum indicates that broader absorption of this mixed polymer than the individual polymers MEH-PPV and MDMO-PPV. The I-V curve indicates that mixture of these two polymers has better I_{sc}, V_{oc} and FF. The V_{oc} and the I_{sc} obtained for the solid-state PEC based on mixture of MEH-PPV and MDMO-PPV photoactive electrode were 289.7 mV and 0.21 μA/ cm^2, respectively under illumination of white light with intensity of 100 mW/cm^2. From transient studies of I_{SC} and V_{OC} small current was observed in the dark. When switching on the light the photocurrent will increase steadily and stays fairly constant for the first on-off and decreases a little to the second on-off experiment and then stable at the photocurrent 0.21 μA/ cm^2 .

The V_{oc} increased sharply with increasing incident light intensity and saturated at higher intensity. The photocurrent of PEC having MEH-PPV:MDMO-PPV as photoactive electrode increases linearly with incident light intensity with power factor, $\alpha = 0.793$. Since $\alpha < 1$, there is recombination by trap. The monochromatic photon to current conversion efficiency under illumination through front side and backside at 490 nm were 0.0034% and 0.00013%, respectively. The photocurrent action spectra study showed that the active junction for the photocurrent generation was that between the photoactive polymer and the redox couple.

In general by mixing two donor polymers (mixture of MEH-PPV and MDMO-PPV) it is possible to increase the optical absorption spectrum of the PEC, which leads to relatively better efficiency.

References

1. M. Green, K. Emery, K. Buecher, D.L. King, S. Igari, *Progress in Photovoltaics, Res. Appl*. **5** (1997) 51

2. T.A. Skotheim, *Handbook of Conducting Polymers*, **Vols. 1, 2,** Marcel Dekker, New York, (1986) PP 125-135.

3. G. Horowitz, *Adv. Mater*. **2** (1990) 287.

4. J. Desilvestro, O. Haas, *J. Chem. Soc., Chem. Commun*. 346 (1985)

5. F.L.C. Miquelino, M.A. De Paoli, E.M. Genie` s, *Synth. Met*. **68** (1994) 91

6. S. Glenis, G. Horowitz, G. Tourillon, F. Garnier, *Thin Solid Films* **93** (1984) 111
7. D. Wokhrle, D. Meissner, *Adv. Mater*. **3** (1991) 129.
8. M. Gerad, A. Chaubey, B.D Malhotra. *(Review), Biosens. Bioelectron*. **17** (2002) 345

9. J.C Vidal, E.G. Ruiz, J.R. Castillo. *Microchim. Acta*. **93** (2003) 143

10. H. Tsumbomura, H. Kobayashi. *Critical Reviews in Solid State and Material Sciences*, **18** 261 (1993)

11. J.L. Bredas, G.B. Street., *Acc.Chem. Res*., **18** (1985) 309.

12. V.V. Waltak., M.M .Labes. Perlstein, *Phys. Rev. Lett*. **31** (1973) 1139

13. W. D .Gill., W. Geiss, R.H., Grant, P.M., R.L. Grene., *Phys. Rev. Lett*., **38** (1977) 1305.

14. H. Shirakawa, E.J. Louis, A.G. MacDiarmid, C.K. Chiang, A.J. Heeger, *J. Chem. Soc. Chem. Comm*., 578 (1977)

15. W.D. Gill., J.C. Clarke, G.B. Street, *Appl. Phys. Commun*., **2** (1982) 211.

16. A .J .Heeger, *J. phys.chem*.B **105,** (2001) 8475

17. G. P. Evans. *Advances in Electrochemical Science and Engineering*, 2 Volumes, Ed. H.Gerischer and C.W. Tobias (1990) PP 1-74

18. P. J. Nigrey, A. G. MacDiarmid, A. J. Heeger, *J. Chem. Soc. Chem. Comm*. **96** (1979) 594

19. G.M. Barrow, *Physical Chemistry* (WCB/McGraw-Hill Boston, Burr Ridge, Dubuque, Madison, New York, San Francisco, St. Louis,), (1996) 6th ed., Chap. 10, 11

20. J.L. Bredas Handbook *of Conducting Polymers*, **Vol. 2**, Ed. T.A. Skotheim, (Marcel Dekker Inc., New York), (1986) Chap. 25, 859

21. R.E. Peierls, *Quantum theory of solids* (Oxford University Press, London) (1955) chap. 5

22. M. Kertesz, J. Koller, A. Azman, *J. Chem. Phys*. **67** (1977) 1189

23. W.P. Su, J. R. Schrieffer, A. J. Heeger, **Phys. Rev. Lett**. **42** (1979) 1698

24. J.L. Bredas, G.B. Street, *Acc. Chem. Res*. **18** (1985), 309

25. J.L. Bredas, D. Beljonne, Z. Shuai, J.M. Toussaint, *Synth. Met*. **41-43** (1991) 3743

26. A. J. Heeger, S. Kivelson, J. R. Schrieffer and W. P. Su, *Rev. mod. Phys*., **60** (1988) 782.

27. M .Tizazu. *Photovoltaic properties of polymer based bulk heterojunction solar cell composed of PDOPT and PCBM*. Addis Ababa university department of physics (2007).

28. S. Kivlson, *Phys. Rev*. B., **25** (1982) 3798.

29. D.E. Fonton, J.MParker, p. v.*write polymer*, **14** (1973) 589

30. M.Armand, M.Dulcot, *French patent,* 7832976, 1978

31. C. Bertier, W.Gorckie, M.B arnand J.m Chabagno, *solid state ionics* ,**11** (2001) 91

32. J.R. Craven, R.H. Mobbs, C. Booth, and J.R.M. Giles, *Makromol. Chem. Rapid Commun.* **7** (1986) 81.

33. F.M. Gray, *Solid State Ionics*, **40** (1990) 637

34. Horowitz, *Adv. Mater*., **2** (1990) 617.

35. A. K. Ghosh and T. Feng, J. *Appl. Phys*., **49** (1978) 5982.

36. D. A Seanor, *Electrical properties of polymers*, Academic Press, New York, (1982)

37. T.A. Skotheim, S.W. Feldberg, and M.B. Armand, *J. Phys. Paris colloq* (1983) 615

38. Reiss, H. and Heller, A., *the absolute potential of the standard hydrogen electrode*: *a new estimate*, J. physics.chem., **89** (1985) 4207

39. A. Gadisa, *Energy Levels in Solar Cells Based on Polymer/Fullerene Bulk Heterojunction*, PhD thesis, Linköping, Sweden, (2006)

40. A. Sergawie, *Solar energy Conversion Based on Organic and Organic/Inorganic hybrid solar cells,* PhD Dissertation, Department of Chemistry, Addis Ababa University, (2007).

41. T. Yohannes, O. Inganäs, *Sol. Energy Materials Sol. Cells* **51** (1998) 193.

42. A. Asrat, A.Sergawie and T. Yohannes, *Solid-state photoelectrochemical solar energy conversion studies based on MEH-PPV and a blend of MEH-PPV with C_{60}* Sinet: Ethiop. J .sci.30(2):85-94, 2007

43. S. Glenis, G. Tourillon, F. Garnier, *Thin Solid Films*, **139** (1986) 221